THE JOURNAL OF BIOLOGICAL CHEMISTRY VOL. 286, NO. 17, pp. 15543–15555, April 29, 2011
Printed in the U.S.A.

Toll-like Receptor 3 Is Required for Development of Retinopathy Caused by Impaired All-*trans*-retinal Clearance in Mice*[S]

Received for publication, February 5, 2011, and in revised form, March 1, 2011 Published, JBC Papers in Press, March 7, 2011, DOI 10.1074/jbc.M111.228551

Satomi Shiose[‡], Yu Chen[‡], Kiichiro Okano[‡], Sanhita Roy[§], Hideo Kohno[‡], Johnny Tang[§¶], Eric Pearlman[§], Tadao Maeda[‡§], Krzysztof Palczewski[‡1], and Akiko Maeda[‡2]

From the Departments of [‡]Pharmacology and [§]Ophthalmology and Visual Sciences, Case Western Reserve University, Cleveland, Ohio 44106 and the [¶]Research Service, Louis Stokes Cleveland Veterans Affairs Medical Center, Cleveland, Ohio 44106

Chronic inflammation is an important component that contributes to many age-related neurodegenerative diseases, including macular degeneration. Here, we report a role for toll-like receptor 3 (TLR3) in cone-rod dystrophy (CORD) of mice lacking ATP-binding cassette transporter 4 (ABCA4) and retinol dehydrogenase 8 (RDH8), proteins critical for all-*trans*-retinal clearance in the retina. Increased expression of toll-like receptor-signaling elements and inflammatory changes were observed in *Rdh8*$^{-/-}$*Abca4*$^{-/-}$ eyes by RNA expression analysis. Unlike 3-month-old *Rdh8*$^{-/-}$*Abca4*$^{-/-}$ mice that developed CORD, 6-month-old *Tlr3*$^{-/-}$*Rdh8*$^{-/-}$*Abca4*$^{-/-}$ mice did not evidence an abnormal retinal phenotype. Light-induced retinal degeneration in *Tlr3*$^{-/-}$*Rdh8*$^{-/-}$*Abca4*$^{-/-}$ mice was milder than that in *Rdh8*$^{-/-}$*Abca4*$^{-/-}$ mice, and a 2-fold increased TLR3 expression was detected in light-illuminated retinas of *Rdh8*$^{-/-}$*Abca4*$^{-/-}$ mice compared with nonilluminated retinas. Poly(I-C), a TLR3 ligand, caused caspase-8-independent cellular apoptosis. Whereas poly(I-C) induced retinal cell death in *Rdh8*$^{-/-}$*Abca4*$^{-/-}$ and WT mice both *in vivo* and *ex vivo*, this was not seen in mice lacking *Tlr3*. Far fewer invasive macrophage/microglial cells in the subretinal space and weaker activation of Muller glial cells were exhibited by *Tlr3*$^{-/-}$*Rdh8*$^{-/-}$*Abca4*$^{-/-}$ mice compared with *Rdh8*$^{-/-}$*Abca4*$^{-/-}$ mice at 3 and 6 months of age, indicating that loss of TLR3 inhibits local inflammation in the retina. Both poly(I-C) and endogenous products emanating from dying/dead retinal cells induced NF-κB and IRF3 activation. These findings demonstrate that endogenous products from degenerating retina stimulate TLR3 that causes cellular apoptosis and retinal inflammation and that loss of TLR3 protects mice from CORD.

Animal models featuring retinal damage to rod/cone photoreceptors have commonly been used to identify and investigate pathogenic mechanisms shared with human blinding diseases. Importantly, mice with defects in the retinoid (visual) cycle needed for continuous regeneration of the visual chromophore, 11-*cis*-retinal (1), have been shown to develop retinal degeneration (2, 3). Such severe cone-rod dystrophy (CORD)[3] develops rapidly in genetically altered mice lacking retinal ATP-binding cassette transporter 4 (ABCA4) and retinol dehydrogenase 8 (RDH8), retinoid cycle proteins involved in clearing all-*trans*-retinal from the retina (4). Specifically, *Rdh8*$^{-/-}$*Abca4*$^{-/-}$ mice initially manifest lipofuscin accumulation, drusen, and photoreceptor/RPE atrophy followed by choroidal neovascularization (CNV) that are hallmark features of human macular degeneration exemplified by Stargardt disease and age-related macular degeneration (AMD). Notably, complement deposition at Bruch membrane in *Rdh8*$^{-/-}$*Abca4*$^{-/-}$ mice may indicate a connection to innate immunity. Not only does the *Rdh8*$^{-/-}$*Abca4*$^{-/-}$ retinal phenotype share many features with human Stargardt disease and AMD, but mutations of the *ABCA4* gene reportedly have a connection with Stargardt disease and susceptibility to AMD (5, 6).

Over the past decade, evidence has accumulated suggesting that aberrant immune responses play an important role in AMD (7–16). Moreover, chronic low grade inflammation could be involved in other age-related diseases, including Alzheimer disease and cardiovascular diseases (17). So, in searching for a link between retinal degeneration in *Rdh8*$^{-/-}$*Abca4*$^{-/-}$ mice and an aberrant immune response, we noted recent reports of an association with the toll-like receptor (TLR) family (18), especially TLR3 (19–21). Recent studies have begun to explore the role of TLRs in retinal innate immunity as well as in the brain (22). Human retinal pigment epithelial (RPE) cells express TLRs with the highest levels reported for TLR3 (19). The latest study demonstrated that stimulation of RPE cells with a synthetic dsRNA could induce the secretion of IFN-β in a TLR3-

* This work was supported, in whole or in part, by National Institutes of Health Grants K08EY019031, K08EY019880, EY009339, EY021126, and P30 EY11373. This work was also supported by a Veterans Affairs Medical Center career development grant, Research to Prevent Blindness Foundation, Foundation Fighting Blindness, and the Ohio Lions Eye Research Foundation.

[S] The on-line version of this article (available at http://www.jbc.org) contains supplemental "Experimental Procedures," Figs. S1–S8, Table 1, and an additional reference.

[1] To whom correspondence may be addressed: Dept. of Pharmacology, School of Medicine, Case Western Reserve University, 10900 Euclid Ave., Cleveland, OH 44106-4965. Tel.: 216-368-4631; Fax: 216-368-1300; E-mail: kxp65@case.edu.

[2] To whom correspondence may be addressed: Depts. of Ophthalmology and Visual Sciences and Pharmacology, School of Medicine, Case Western Reserve University, 10900 Euclid Ave., Cleveland, OH 44106-7286. Tel.: 216-368-0670; Fax: 216-368-1300; E-mail: aam19@case.edu.

[3] The abbreviations used are: CORD, cone-rod dystrophy; A2E, di-retinoid-pyridinium-ethanolamine; AMD, age-related macular degeneration; ERG, electroretinogram; GFAP, glial fibrillary acidic protein; poly(I-C), polyinosinic-:polycytidylic acid or polyinosinic-polycytidylic acid sodium salt; RPE, retinal pigment epithelium; SD-OCT, spectral domain optical coherence tomography; SLO, scanning laser ophthalmoscopy; TLR, toll-like receptor; CNV, choroidal neovascularization; TIR, Toll/IL-1 receptor; TRIF, TIR domain-containing adapter-inducing interferon-β; dsRNA, double-stranded RNA; qPCR, quantitative PCR; Ab, antibody; h, human.

dependent manner and that these RPE cells in turn were responsive to the antiviral action of IFN-β. Furthermore, TLR3 stimulation of RPE cells induced the secretion of various cytokines, chemokines, and adhesion molecules. Poly(I-C), a synthetic dsRNA, induced apoptosis via TLR3 in both human and mouse RPE cells (20, 21). Thus, TLR3-mediated signaling triggered by dsRNA might play a role in retinal diseases. These observations led to the present investigation describing the participation of TLR3 in the pathogenesis of CORD in *Rdh8*$^{-/-}$*Abca4*$^{-/-}$ mice.

Here, we investigated the role of TLR3 in the development of retinopathy in *Rdh8*$^{-/-}$*Abca4*$^{-/-}$ mice as compared with *Tlr3*$^{-/-}$*Rdh8*$^{-/-}$*Abca4*$^{-/-}$ mice. We also investigated dsRNA-induced RPE apoptosis and local inflammation using cell culture experiments. Our results demonstrate that TLR3 deficiency protects the retina from age-related and light-induced degeneration in *Rdh8*$^{-/-}$*Abca4*$^{-/-}$ mice. Interestingly, endogenous products from dying/dead retinal cells due to elevated concentrations of all-*trans*-retinal caused TLR3-dependent cellular apoptosis and inflammation, whereas all-*trans*-retinal, implicated in the pathogenesis of retinal degeneration in *Rdh8*$^{-/-}$*Abca4*$^{-/-}$ mice, did not activate TLR3. Together, these observations implicate TLR3 activation in the blinding retinopathy observed in *Rdh8*$^{-/-}$*Abca4*$^{-/-}$ mice.

EXPERIMENTAL PROCEDURES

Animals—*Rdh8*$^{-/-}$*Abca4*$^{-/-}$ double knock-out mice were generated as described previously, and all knock-out mice were genotyped by established methods (4, 23). *Tlr3*$^{-/-}$*Rdh8*$^{-/-}$*Abca4*$^{-/-}$ triple knock-out mice were generated by cross-breeding *Rdh8*$^{-/-}$*Abca4*$^{-/-}$ double knock-out mice with *Tlr3*$^{-/-}$ mice. *Tlr3*$^{-/-}$ mice were kindly provided by Dr. Shizuo Akira (Research Institute for Microbial Disease, Osaka University, Osaka, Japan). These animals and their progeny were genotyped by PCR with the following primers: WT fragment (1 kb), forward 5′-CCAGAGCCTGGGTAAGTTATTGTGCTG-3′ and reverse 5′-TCCAGACAATTGGCAAGTTATTCGCCC-3′; KO fragment (1 kb), forward 5′-TCCAGACAATTGGCAAGTTATTCGCCC-3′ and reverse 5′-ATCGCCTTCTATCGCCTTCTTGACGAG-3′. Only mice with the leucine variation at amino acid 450 of RPE65 were used. All mice were housed in the animal facility at the School of Medicine, Case Western Reserve University, where they were maintained either under complete darkness or in a 12-h light (~10 lux)/12-h dark cycle environment. Experimental manipulations in the dark were done under dim red light transmitted through a Kodak No. 1 safelight filter (transmittance >560 nm). All animal procedures and experiments were approved by the Case Western Reserve University Animal Care Committees and conformed to both the recommendations of the American Veterinary Medical Association Panel on Euthanasia and the Association of Research for Vision and Ophthalmology.

RNA Expression Analysis—RNA expression analysis was performed by RT^2 Profiler PCR array system provided by SABiosciences (Frederick, MD). Total RNA from mouse eyes was purified by RiboPure kit (Ambion, Austin, TX). Fold changes were normalized to five housekeeping genes (Tables 1 and 2).

Primary RPE Cell Cultures—Primary mouse retinal pigment epithelial (RPE) cells were isolated from mouse eyes by a published method (24) with modifications described in the supplemental material.

Ultra-high Resolution Spectral Domain Optical Coherence Tomography (SD-OCT) and Scanning Laser Ophthalmoscopy (SLO) Imaging—Ultra-high resolution SD-OCT (Bioptigen, Research Triangle Park, NC) and HRAII (Heidelberg Engineering, Germany) for SLO were employed for *in vivo* imaging of mouse retinas. Mice were anesthetized by intraperitoneal injection of a mixture (20 μl/g body weight) containing ketamine (6 mg/ml) and xylazine (0.44 mg/ml) in 10 mM sodium phosphate, pH 7.2, with 100 mM NaCl. Pupils were dilated with 1% tropicamide. Four pictures acquired in the B-scan mode were used to construct each final averaged SD-OCT image.

Retinoid and A2E Analyses—All experimental procedures related to extraction, derivatization, and separation of retinoids from dissected mouse eyes were carried out as described previously (23). For A2E extraction, two eyes were homogenized in 1 ml of acetonitrile in a glass/glass homogenizer. After evaporation of solvent, extracts were dissolved in 150 μl of acetonitrile with 0.1% trifluoroacetic acid (TFA) and then passed through a Teflon syringe filter (National Scientific Co., Quakertown, PA). Samples (100 μl) were loaded on C18 columns (Phenomenex, Torrance, CA) and analyzed by normal phase HPLC with a mobile phase gradient of acetonitrile/H_2O, 100:0, and acetonitrile/H_2O, 80:20, with 0.1% TFA for 30 min. Quantification of A2E by HPLC was performed by comparison with known concentrations of pure synthetic A2E prepared as described previously (25).

Histology—Histological and immunohistochemical procedures employed were well established (23). Anti-rhodopsin 1D4 antibody was a generous gift from Dr. R. S. Molday (University of British Columbia, Vancouver). Anti-TLR3 polyclonal antibody was purchased from Santa Cruz Biotechnology, and anti-macrophage antibodies, CD11b and F4/80, were obtained from AbD Serotec (Raleigh, NC). Anti-GFAP antibody was purchased from DAKO (Glostrup, Denmark). Eyecups for histology were fixed in 2% glutaraldehyde, 4% paraformaldehyde and processed for embedding in Epon. Sections were cut at 1 μm and stained with toluidine blue (23).

ERG—All ERG procedures were performed by published methods (23). For single-flash recording, the duration of white light flash stimuli (from 20 μs to 1 ms) was adjusted to provide a range of illumination intensities (from −3.7 to 1.6 log candela·s/m^2). Three to five recordings were made at sufficient intervals between flash stimuli (from 10 s to 10 min) to allow recovery from any photobleaching effects.

Mouse Fundus Images—Retinal fundus images were obtained by using a surgical microscope (Leica M651 MSD, Werzlar, Germany) connected to a CCD camera. Aberrant reflection from the cornea was removed by a HOYA HHV Dispo type-6d lens (HOYA, Tokyo, Japan).

RPE Cell Death Induced by Synthesized TLR3 Ligand, Poly(I-C)—ARPE19 cells and primary RPE cells from *Tlr3*$^{-/-}$*Rdh8*$^{-/-}$*Abca4*$^{-/-}$, *Rdh8*$^{-/-}$*Abca4*$^{-/-}$, *Tlr3*$^{-/-}$, *Trif*$^{-/-}$, and

WT mice were cultured in 24-well plates at a density of 5×10^4 cells per well (60–70% confluence). RPE cells were co-incubated with various concentrations (20, 50, 100, and 200 μg/ml) of poly(I-C) for 24 h at 37 °C. After co-incubation, RPE cells were stained with Hoechst 33342 (AnaSpec Inc., Fremont, CA) for 30 min and washed twice with phosphate-buffered saline (PBS: 137 mM NaCl, 2.7 mM KCl, 4.3 mM Na_2HPO_4, 1.4 mM KH_2PO_4). Evaluation of cell death was performed by counting the number of cells with nuclei densely stained by Hoechst 33342 dye under a fluorescent microscope (Leica DMI 6000 system). ARPE19 cells were maintained in medium (Dulbecco's modified Eagle's medium (DMEM) with 10% fetal calf serum), and the α-minimal essential medium modification (Invitrogen) with 10% fetal calf serum was used for primary RPE cells.

RPE Cell Death Induced by Products from Degraded Retinal Cells—Y79 cells (derived from human retinoblastoma) were seeded into 24-well plates at a density of 1×10^5 cells/well in 500 μl of DMEM with 10% fetal calf serum and treated with 30 μM all-*trans*-retinal for 16 h at 37 °C to cause cell death in the presence of 400 units/ml RNase inhibitor (Invitrogen or New England Biolabs). Then Y79 cells after co-incubation with all-*trans*-retinal were exposed to UV light (365 nm; 8-watt UV lamp from UVP, Inc.) for 15 min to destroy all-*trans*-retinal, and the culture supernatants, including products from degraded Y79 cells, were collected by centrifugation at 12,500 rpm for 5 min. ARPE19 cells (5×10^4 cells/well in a 24-well plate) were co-incubated with the resulting supernatants for 24 h at 37 °C, and cell viability was quantified as described above. RNase A (for single-stranded RNA), RNase H (for RNA-DNA complex), RNase III (for rRNA and dsRNA), and DNase I were purchased from New England Biolabs (Ipswich, MA), and Benzonase® was bought from Sigma. Twenty units/ml of these nucleases were used for co-incubation with products from degraded Y79 cells. All-*trans*-retinal was obtained from Toronto Research Chemicals, Inc. (Toronto, Canada).

Subretinal Injection of Poly(I-C)—All surgical manipulations were conducted under a surgical microscope (Leica M651 MSD). Mice were anesthetized by intraperitoneal injection of 20 μl/g of body weight of 6 mg/ml ketamine and 0.44 mg/ml xylazine diluted with 10 mM sodium phosphate, pH 7.2, containing 100 mM NaCl. Pupils were dilated with 1.0% tropicamide ophthalmic solution (Bausch & Lomb, Rochester, NY). A 33-gauge beveled needle (World Precision Instruments, Sarasota, FL) was used as a lance to make a full thickness cut through sclera at 1.0 mm posterior to the limbus. This was replaced with a 36-gauge beveled needle attached to an injection system (UMP-II microsyringe pump and Micro4 controller with a footswitch, World Precision Instruments). The needle was aimed toward the inferior nasal area of retina, and a poly(I-C) solution (Invivogen, 1 μg in 1.0 μl of PBS) was injected into the subretinal space. Successful administration was confirmed by observing bleb formation. The tip of the needle remained in the bleb for 10 s after bleb formation, and the needle was then gently withdrawn. As a control, saline was injected into the subretinal space by the same procedure.

NF-κB and IRF3 Reporter Assay—Human TLR3 cDNA (pUNO-hTLR3-GFP, Invivogen) was transfected into ARPE19 cells to obtain stable hTLR3-expressing ARPE19 cells (hTLR3-ARPE19). ARPE19, hTLR3-ARPE19, HEK293 (with TLR3 undetectable by our RT-PCR method), and hTLR3-HEK293 cells were transfected with either an NF-κB reporter plasmid possessing a secreted alkaline phosphatase (pNiFty2-SEAP) (Invivogen) or 561-luc for IRF3 reporter plasmid (generous gift from Dr. Xiaoxia Li, Cleveland Clinic Foundation, Cleveland, OH) by using Lipofectamine2000 (Invitrogen) 24 h before co-incubation with the TLR3 ligand. HEK-Blue detection (Invivogen) was used to assay for secreted alkaline phosphatase production according to the manufacturer's protocol. The luciferase assay was performed with a Dual-Luciferase reporter assay system (Promega, Madison, WI).

Translocation of p65 to the Nucleus—Bone marrow cells were derived from 6- to 8-week-old C57BL/6, *Tlr3*$^{-/-}$, *Trif*$^{-/-}$ and *Tlr9*$^{-/-}$ mice. Following euthanasia by CO_2 asphyxiation, femurs and tibias were removed, and the shafts were centrifuged at 10,000 rpm for 30 s at 4 °C. The pellet was resuspended in 1 ml of sterile RBC lysis buffer (Ebioscience, San Diego) for 2–3 min, and cells were centrifuged at 1,200 rpm for 5 min at room temperature and then washed once using sterile DMEM. Cells were incubated in DMEM containing 10% FBS and 30% L929-conditioned medium for 10 days to differentiate them into macrophages (26). The resulting cells (5×10^4) were cultured on sterile coverslips in 24-well plates and stimulated for 0, 15, 30, 60, and 120 min with either LPS (100 ng/ml), poly(I-C) (10 μg/ml), or supernatants containing degraded Y76 cells obtained after a 16-h co-incubation with 30 μM all-*trans*-retinal. Following activation, the cells were fixed with 4% paraformaldehyde for 15 min at room temperature. Fixed cells were permeabilized with 0.1% Triton X-100 in PBS for 1 min at room temperature and incubated with rabbit anti-mouse p65 (1:100; Ebioscience) in PBS containing 10% goat serum for 1 h at room temperature. Coverslips were washed twice with PBS and incubated with Alexa Fluor 488-labeled goat anti-rabbit IgG Ab (Invitrogen) in PBS at room temperature for 1 h, washed with PBS, and placed on glass slides using Vectashield mounting medium with DAPI (Vector Laboratories, Peterborough,UK). Images were captured with a Leica DMI 6000 B inverted microscope connected to a Retiga EXI camera (Q-imaging, Vancouver, British Columbia, Canada).

Statistical Analyses—Data representing the means ± S.D. or the means ± S.E. for the results of at least three independent experiments were compared by the one-way analysis of variance test.

RESULTS

TLR Signaling Is Enhanced in Retinal Degeneration Exhibited by Rdh8$^{-/-}$*Abca4*$^{-/-}$ *Mice*—TLRs constitute distinct families of pattern-recognition receptors that recognize components derived from viruses or endogenous cellular degradation and trigger innate immune responses (18). To study the putative role of TLRs in retinal degeneration, we performed expression analysis of 84 genes involved in TLR signaling and 5 housekeeping genes with RNA extracted from *Rdh8*$^{-/-}$*Abca4*$^{-/-}$ mouse eyes. Retinal degeneration develops CORD in *Rdh8*$^{-/-}$*Abca4*$^{-/-}$ mice that becomes apparent at 6 weeks of age, and 3-month-old *Rdh8*$^{-/-}$*Abca4*$^{-/-}$ mice display widespread degeneration of the inferior retina (4). Eventually, some

TABLE 1

mRNA expression profiling of eyes from *Rdh8*$^{-/-}$*Abca4*$^{-/-}$ mice for molecules in the TLR signaling pathway

Fold changes only greater than 2 are presented. The data was normalized to the housekeeping genes (*Gusb, Gapdh, Actb, Hprt1*, and *Hsp90ab1*).

	Light/dark (6–8-month-old)[a]		2–4-month-old/6–8-month-old[b]	
	Genes	-Fold	Genes	-Fold
Toll-like receptors				
	Tlr2	5.58	*Tlr2*	8.25
	Tlr8	5.07	*Tlr5*	7.74
	Tlr5	4.05	*Tlr3*	4.07
	Tlr3	3.80	*Tlr8*	3.85
	Tlr4	2.09	*Tlr4*	3.04
			Tlr1	2.16
	Tlr6[c]	−2.08	*Tlr6*	−2.06
Adaptors TLR-interacting proteins				
	Hras1	6.93	Hras1	8.72
	Mapk8ip3	6.81	*Mapk8ip3*	7.11
	Trif	5.85	*Myd88*	5.74
	Peli1	5.05	*Trif*	5.73
	Myd88	3.49	*Peli1*	4.56
	Pglyrp1	3.37	*Tirap*	3.54
	Tollip	2.55	*Tram*	3.39
			Pglyrp1	2.96
			Tollip	2.30
Effectors				
	Traf6	14.83	*Traf6*	12.72
	Tnfrsf1a	11.16	*Irak2*	5.15
	Nr2c2	4.30	*Ppara*	4.31
	Irak2	3.89	*Ube2v1*	4.16
	Ppara	3.89	*Nr2c2*	3.74
	Ube2v1	3.86	*Map3k7*	2.02
			Casp8	2.01
Downstream pathways and target genes				
NF-κB pathway	*Rela*	6.65	*Tnfrsf1a*	14.16
	Nfrkb	5.68	*Nfkb2*	6.67
	Tnfaip3	5.41	*Rela*	6.56
	Ikbkb	5.16	*Tnfaip3*	6.42
	Tnf	4.58	*Nfkbil1*	5.64
	Nfkbil1	3.83	*Ikbkb*	5.49
	Nfkb2	3.71	*Nfrkb*	4.90
	Hrb	3.40	*Il12a*	4.32
	Il12a	3.31	*Hrb*	3.28
	Nfkbia	2.97	*Nfkbia*	3.02
	Nfkb1	2.56	*Map3k1*	3.00
	Il10	2.55	*Tnf*	2.92
	Ifng	2.10	*Nfkb1*	2.83
	Rel	2.05	*Il10*	2.80
			Ifng	2.37
			Il1r1	2.19
	Il1b	−2.32		
JNK/p38 pathway	*Fos*	5.68	*Jun*	5.46
	Jun	4.50	*Elk1*	3.90
	Elk1	4.14	*Mapk8*	3.46
	Mapk9	4.06	*Mapk9*	2.88
	Mapk8	3.05		
	Map3k7	2.01		
NF/IL6 pathway	*Ptgs2*	5.07	*Ptgs2*	3.78
	Il6ra	2.59	*Il6ra*	2.47
IRF pathway	*Irf3*	6.74	*Irf3*	6.20
	Irf1	3.71	*Irf1*	4.61
	Tbk1	3.09	*Tbk1*	3.16
	Cxcl10	−5.53	*Cxcl10*	−2.62
	Ifnb	−2.72		
Regulation of adaptive immunity				
	Cd80	2.86	*Cd80*	2.57

[a] *Rdh8*$^{-/-}$*Abca4*$^{-/-}$ mice at the ages of 6–8 months were used. Mice were maintained either under a 12-h light (10 lux)/12-h dark cycle or kept in the dark.
[b] *Rdh8*$^{-/-}$*Abca4*$^{-/-}$ mice at the ages of 2–4 or 6–8 months were used. Animals were maintained under a 12-h light (10 lux)/12-h dark cycle.
[c] Minus signs together with underlining indicate reduced expression.

Rdh8$^{-/-}$ *Abca4*$^{-/-}$ mice develop CNV at 6 months of age or older. No obvious retinal degeneration was noted if *Rdh8*$^{-/-}$ *Abca4*$^{-/-}$ mice were kept in the dark. In this study, *Tlr*-related mRNA expression was assessed in retinas of 6–8-month-old *Rdh8*$^{-/-}$ *Abca4*$^{-/-}$ mice maintained either under regular laboratory lighting conditions (light) or in the dark (dark) to compare degenerated with nondegenerated retinas and in young 2–4-month-old and aged 6–8-month-old *Rdh8*$^{-/-}$*Abca4*$^{-/-}$ mice maintained under regular laboratory light to contrast early degenerating retinas with more severely degenerated retinas featuring CNV (Table 1). Interestingly, expression levels of mRNA encoding molecules involved in TLR signaling, including TLRs themselves, were higher in the retinas of light-kept than dark-kept *Rdh8*$^{-/-}$*Abca4*$^{-/-}$ mice, and young *Rdh8*$^{-/-}$

TABLE 2
Changes in mRNA expression profiling in eyes from C57BL/6J wild-type mice alone and compared with changes in eyes from *Rdh8*$^{-/-}$ *Abca4*$^{-/-}$ mice

WT 6–8-month-old/WT 2–4-month-old		DKO/WT (2–4-month-old)[a]		DKO/WT (6–8-month-old)[a]	
Genes	-Fold[b]	Genes	-Fold[c]	Genes	-Fold[c]
Cxcl10	3.08	*Ifnb*	31.42	*Ifnb*	29.35
Tlr3	2.88	*Ifng*	6.31	*Cxcl10*	3.11
Trif	2.14	*Cxcl10*	3.65		

[a] DKO indicates double knock-out *Rdh8*$^{-/-}$*Abca4*$^{-/-}$ mice.
[b] Fold changes greater than 2 are presented. The data was normalized to the housekeeping genes (*Gusb, Gapdh, Actb, Hprt1,* and *Hsp90ab1*).
[c] Ratios greater than 3-fold are presented. Toll-like receptors did not show changes greater than 3-fold.

Abca4$^{-/-}$ mice showed a higher expression of these mRNAs than older *Rdh8*$^{-/-}$*Abca4*$^{-/-}$ mice. Following ligand binding, TLRs recruit a specific combination of intracellular Toll/IL-1 receptor (TIR) domain-containing adaptors to the TIR region. These include the myeloid differentiation primary response gene 88 (*MyD88*), TIR-containing adaptor protein, TIR domain-containing adapter-inducing interferon-β (TRIF)/TIR domain-containing adaptor molecule 1 (TICAM1), and TRIF-related adaptor molecule (TRAM)/TICAM2 (27). Table 1 shows that increased expression of mRNA encoding these adaptors was noted in the retinas of young and old light-kept *Rdh8*$^{-/-}$*Abca4*$^{-/-}$ mice. Elevated mRNA expression of TLR effectors, including TRAF6, and downstream targets such as NF-κB, MAPK, and IRF3 also were detected in these mice. These data strongly suggest that TLRs are involved in the pathology of CORD in *Rdh8*$^{-/-}$*Abca4*$^{-/-}$ mice. Furthermore, age-related inflammation with elevated CXCL10 chemokine, TLR3, and TRIF expression was discovered in WT mice as well (Table 2).

Expression of TLRs in Rdh8$^{-/-}$*Abca4*$^{-/-}$ *Retina, Primary Cultured Rdh8*$^{-/-}$*Abca4*$^{-/-}$ *RPEs, and ARPE19 Cells*—To determine whether TLRs (*Tlr2*, *Tlr3*, *Tlr4*, *Tlr5,* and *Tlr8*) are expressed in the retina/RPE after increased expression was noted in the array analysis of whole eyes (Table 1), we performed RT-PCR with RNAs derived from whole eyes, dissected retina, and primary cultured RPE cells from 4-week-old *Rdh8*$^{-/-}$*Abca4*$^{-/-}$ mice. RT-PCR demonstrated that retina (including RPE), whole eyes, and primary cultured RPE cells of *Rdh8*$^{-/-}$*Abca4*$^{-/-}$ mice expressed all of these *Tlrs* (supplemental Table S1). RT-PCR of the RPE and photoreceptor-specific proteins, RPE65 and rhodopsin, demonstrated that there was no contamination of the primary cultured RPE cells with photoreceptors. Expression of TLR3 and TLR4 in ARPE19 cells was subsequently detected by RT-PCR as reported previously (19, 28).

Absence of TLR3 Protects against Retinal Degeneration in Rdh8$^{-/-}$*Abca4*$^{-/-}$ *Mice—Rdh8*$^{-/-}$*Abca4*$^{-/-}$ mice displayed retinal degeneration with reduced thickness of rod photoreceptor outer segments, mislocalization of rhodopsin, and loss of cone photoreceptors by the age of 3 months, and these changes became more severe in 6-month-old *Rdh8*$^{-/-}$*Abca4*$^{-/-}$ mice, establishing that these mice show progressive retinal degeneration as reported previously (Fig. 1*A*) (4). In contrast, *Tlr3*$^{-/-}$*Rdh8*$^{-/-}$*Abca4*$^{-/-}$ mice failed to exhibit apparent retinal damage by the age of 6 months, similar to *Tlr3*$^{-/-}$ or WT mice. ERGs showed reduced amplitudes of a- and b-waves in *Rdh8*$^{-/-}$*Abca4*$^{-/-}$ mice at the age of 6 months as compared with WT mice of the same age, whereas no significant changes were detected between 6-month-old *Tlr3*$^{-/-}$*Rdh8*$^{-/-}$*Abca4*$^{-/-}$ mice and WT mice (Fig. 1*B*). These data indicate that deletion of TLR3 protected against the age-related retinal degeneration noted in *Rdh8*$^{-/-}$*Abca4*$^{-/-}$ mice.

Deletion of TLR3 Protects Retinas from Light-induced Acute Degeneration—In addition to developing age-related retinal degeneration displaying CORD, *Rdh8*$^{-/-}$*Abca4*$^{-/-}$ mice manifest acute retinal degeneration after bright light exposure. To study the role of TLR3 in light-induced acute retinal degeneration, we illuminated *Rdh8*$^{-/-}$*Abca4*$^{-/-}$ and *Tlr3*$^{-/-}$*Rdh8*$^{-/-}$*Abca4*$^{-/-}$ mice with 10,000 lux light for 15, 30, and 60 min. Because the light intensity of sunny outside Cleveland, OH, reaches more than 80,000 lux, the intensity used here was strong but still physiological. *Rdh8*$^{-/-}$*Abca4*$^{-/-}$ mice demonstrated significant retinal damage by 15 min of such exposure (data not shown) (29), and 30 min of illumination destroyed ~50% of the photoreceptors in the central part of the retina (Fig. 2*A*). In contrast, *Tlr3*$^{-/-}$*Rdh8*$^{-/-}$*Abca4*$^{-/-}$ mice showed severe retinal degeneration similar to *Rdh8*$^{-/-}$*Abca4*$^{-/-}$ mice only after 60 min of such exposure. Consistently, we failed to detect subretinal autofluorescent spots in *Tlr3*$^{-/-}$*Rdh8*$^{-/-}$*Abca4*$^{-/-}$ mice by an SLO, whereas increased numbers were readily identified in *Rdh8*$^{-/-}$*Abca4*$^{-/-}$ mice after 30 min of illumination, an exposure that failed to cause retinal degeneration in WT mice (Fig. 2*B*). Increased numbers of subretinal autofluorescent spots were found in both *Tlr3*$^{-/-}$*Rdh8*$^{-/-}$*Abca4*$^{-/-}$ and *Rdh8*$^{-/-}$*Abca4*$^{-/-}$ mice exposed to 60 min illumination (data not shown). Because elevated expression of TLRs was seen during development of age-related retinal degeneration in *Rdh8*$^{-/-}$*Abca4*$^{-/-}$ mice (Table 1), TLR3 expression was assessed by both conventional RT-PCR and quantitative PCR (qPCR). *Rdh8*$^{-/-}$*Abca4*$^{-/-}$ mice were illuminated with 10,000 lux for 60 min, and their retinas were promptly collected because loss of photoreceptors is not obvious immediately after illumination. Actually, the processes of apoptosis and removal of dead/dying cells from the retina takes 5–7 days after this insult (29). Conventional RT-PCR demonstrated increased TLR3 expression in light-illuminated retinas compared with nonilluminated retinas (Fig. 2*C*). qPCR then confirmed that light-illuminated retinas showed a 2-fold increase in TLR3 expression relative to nonilluminated retinas.

RPE Cell Death Is Caused by TLR3-activating Ligand in Vitro—We next investigated the role of TLR3 in photoreceptor/RPE cell death. Our rationale included the reported differential susceptibility to AMD noted in TLR3 polymorphisms (20), prominent TLR3 expression in the RPE (19), and TLR3-induced retinal cell

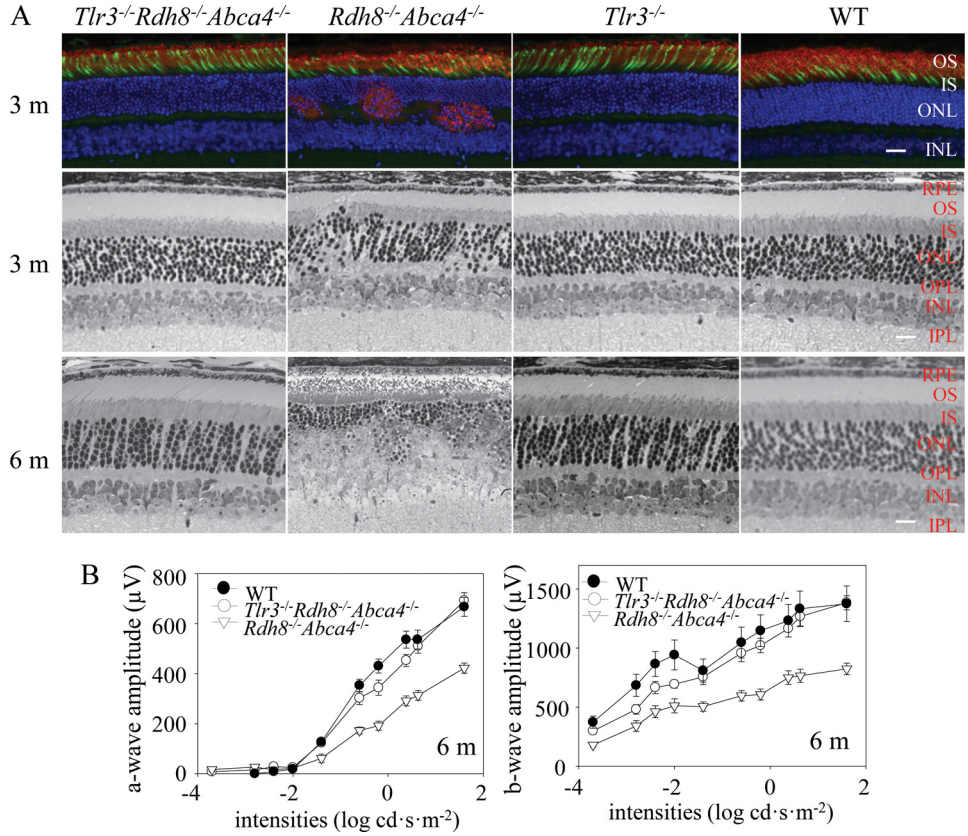

FIGURE 1. **Deletion of *Tlr3* protects against developing retinal degeneration in *Rdh8*$^{-/-}$*Abca4*$^{-/-}$ mice.** *A,* retinal morphology was examined in *Tlr3*$^{-/-}$*Rdh8*$^{-/-}$*Abca4*$^{-/-}$, *Rdh8*$^{-/-}$*Abca4*$^{-/-}$, *Tlr3*$^{-/-}$, and WT mice at the ages of 3 and 6 months (*m*). Cryosections from 3-month-old mice were stained with anti-rhodopsin Ab (*red*), peanut agglutinin lectin (*green*), and 4′-6-diamidino-2-phenylindole (*blue*) (*top panel*). Epon-prepared retinas of 3- and 6-month-old mice also are shown (*middle* and *lower panels*). Significant retinal degeneration with rhodopsin mislocalization occurred in *Rdh8*$^{-/-}$*Abca4*$^{-/-}$ mice, whereas the other mice did not show obvious retinal damage. *Bars* indicate 10 μm. *OS*, outer segment; *IS*, inner segment; *ONL*, outer nuclear layer; *INL*, inner nuclear layer; *RPE,* retinal pigment epithelium; *OPL,* outer plexiform layer; *IPL,* inner plexiform layer. *B,* full field ERG responses of WT, *Tlr3*$^{-/-}$*Rdh8*$^{-/-}$*Abca4*$^{-/-}$, and *Rdh8*$^{-/-}$*Abca4*$^{-/-}$ mice at 6 months of age. ERG responses were recorded under scotopic conditions. Both a- (*left*) and b- (*right*) wave amplitudes plotted as a function of light intensity were significantly attenuated in 6-month-old *Rdh8*$^{-/-}$*Abca4*$^{-/-}$ mice as compared with *Tlr3*$^{-/-}$*Rdh8*$^{-/-}$*Abca4*$^{-/-}$ and WT animals. *Bars* indicate S.E. of the means ($n > 6$; *, $p < 0.01$), *Rdh8*$^{-/-}$*Abca4*$^{-/-}$ mice *versus Tlr3*$^{-/-}$*Rdh8*$^{-/-}$*Abca4*$^{-/-}$ animals. *cd*, candela.

death (20, 21), as well as our own findings that TLR3 expression was increased in older WT mice and *Rdh8*$^{-/-}$ *Abca4*$^{-/-}$ mice with retinal degeneration (Table 1) and that ablation of *Tlr3* protected against retinal degeneration in *Rdh8*$^{-/-}$*Abca4*$^{-/-}$ mice (Figs. 1 and 2).

ARPE19 cells expressing TLR3 were co-incubated with the TLR3-activating ligand poly(I-C) at various concentrations for 24 h, after which cells were stained with Hoechst 33342 to assess cellular apoptosis. Interestingly, increasing numbers of these cells showing chromatin condensation were noted in a dose-dependent manner (Fig. 3, *A* and *B*). Expression of caspase-8, p53, and Bax was determined by immunoblot, because caspase-8/TLR3-dependent apoptotic cell death had been reported (30). Surprisingly, the immunoblot did not reveal any caspase-8 in ARPE19 cells. Elevated Bax expression indicates that poly(I-C) induced Bax-dependent but caspase-8-independent apoptosis in ARPE19 cells. HEK293 cells displayed poly(I-C)-induced caspase-8 activation (cleavage of full-length of caspase-8) as reported (supplemental Fig. S1).

To characterize further the TLR3-dependent RPE cell death induced by the TLR3 ligand poly(I-C), primary RPE cells were first isolated from *Tlr3*$^{-/-}$*Rdh8*$^{-/-}$*Abca4*$^{-/-}$, *Rdh8*$^{-/-}$*Abca4*$^{-/-}$, *Tlr3*$^{-/-}$, and WT mice, and then poly(I-C) was mixed into the cell culture media. As expected, significant poly(I-C)-induced cell death was observed in RPE cells from *Rdh8*$^{-/-}$*Abca4*$^{-/-}$ and WT mice but not from *Tlr3*$^{-/-}$*Rdh8*$^{-/-}$*Abca4*$^{-/-}$ or *Tlr3*$^{-/-}$ mice (Fig. 3*C*). These data provide evidence that activation of TLR3 by artificial dsRNA poly(I-C) can induce RPE cell apoptosis. In addition, primary RPE from *Trif*$^{-/-}$ mice showed significantly less poly(I-C)-induced cell death, indicating that TLR3 and TRIF also participate in producing such cell death.

Subretinal Injection of Poly(I-C) Induces Retinal Degeneration in Mice—Because poly(I-C) caused death of ARPE19 cells and primary cultured RPE cells from mice in a TLR3-dependent manner, poly(I-C) (1 μl of 1 μg/μl in PBS) was injected subretinally into 8-week-old WT, *Tlr3*$^{-/-}$, and *Trif*$^{-/-}$ mice to investigate TLR3-dependent events *in vivo*. Retinal morphology was examined by spectral domain optic coherence tomography (SD-OCT) at 1, 2, and 4 weeks after injection. Retinal detachment due to the subretinal injection occurred up to 1–2 weeks after injection in most treated eyes (supplemental Fig. S2*A*). Importantly, widespread severe retinal degeneration was seen in poly(I-C)-injected WT retinas, whereas only regional degeneration caused by needle damage at the injected site was observed in *Tlr3*$^{-/-}$ and *Trif*$^{-/-}$ mice 4 weeks after the injec-

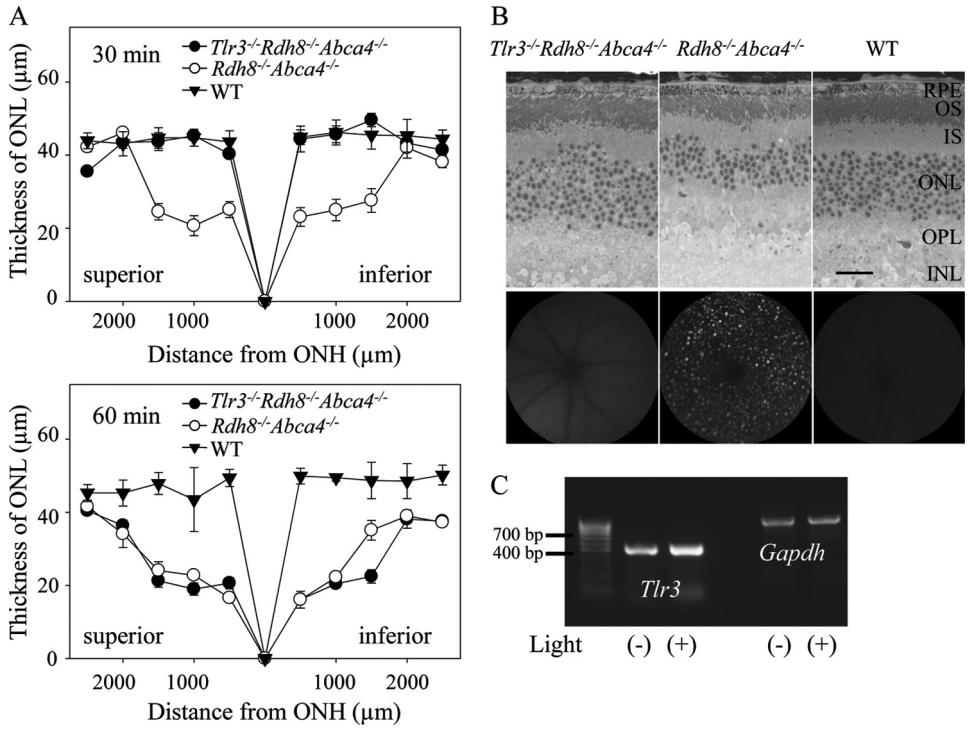

FIGURE 2. **Tlr3 deletion protects retinas from light-induced acute degeneration.** *Tlr3*$^{-/-}$*Rdh8*$^{-/-}$*Abca4*$^{-/-}$, *Rdh8*$^{-/-}$*Abca4*$^{-/-}$, and WT mice at 4 weeks of age were exposed to 10,000 lux light for 30 and 60 min and then kept in the dark for 7 days when SLO and histological examinations were performed. *A,* thickness of the outer nuclear layer (*ONL*) is shown. *ONH,* optic nerve head. *Error bars* indicate S.D. of the means ($n > 3$). Severe retinal degeneration was observed in *Rdh8*$^{-/-}$*Abca4*$^{-/-}$ mice after bright light exposure for 30 min, whereas no degeneration was detected in *Tlr3*$^{-/-}$*Rdh8*$^{-/-}$*Abca4*$^{-/-}$ and WT retinas. However, severe light-induced retinal degeneration was noted in both *Tlr3*$^{-/-}$*Rdh8*$^{-/-}$*Abca4*$^{-/-}$ mice and *Rdh8*$^{-/-}$*Abca4*$^{-/-}$ mice after 60 min of bright light exposure. *B, upper panel,* retinal histology of 30-min light-illuminated mice is shown. *RPE,* retinal pigment epithelium; *OS,* outer segments; *IS,* inner segments; *ONL,* outer nuclear layer; *OPL,* outer plexiform layer; *INL,* inner nuclear layer. *Bar* indicates 20 μm. *Lower panel,* representative outer retinal images obtained by SLO of 4-week-old mice 7 days after exposure to 10,000 lux light for 30 min are presented. Numerous autofluorescent deposits seen in illuminated *Rdh8*$^{-/-}$*Abca4*$^{-/-}$ mice were absent in *Tlr3*$^{-/-}$*Rdh8*$^{-/-}$*Abca4*$^{-/-}$ and WT mice. *C,* RT-PCR for *Tlr3* and a *Gapdh* internal control from retinas of illuminated and nonilluminated *Rdh8*$^{-/-}$*Abca4*$^{-/-}$ mice are shown. Expression of *Tlr3* increased after bright light exposure.

tion (Fig. 4*A* and supplemental Fig. S2). Injection of vehicle (PBS) produced only local retinal damage, similar to that observed in poly(I-C)-injected *Tlr3*$^{-/-}$ and *Trif*$^{-/-}$ retinas. Furthermore, widespread retinal atrophy was evident in fundus images of poly(I-C)-injected WT retinas (Fig. 4*B*). These results provide evidence that poly(I-C) causes retinal degeneration via TLR3/TRIF *in vivo* and that this pathway is involved in the progression of certain types of retinal degeneration in mice.

TLR3$^{-/-}$*Rdh8*$^{-/-}$*Abca4*$^{-/-}$ *Mice Exhibit Decreased Numbers of Autofluorescent Subretinal Macrophage/Microglia and a Weaker Retinal Inflammatory Response*—Increasing evidence indicates that autofluorescent subretinal macrophages and microglial cells accumulate during aging and light-induced retinal degeneration (31–33). Here, we examined retinas for these cells with an SLO. Although autofluorescent spots increased with age in both *Tlr3*$^{-/-}$*Rdh8*$^{-/-}$*Abca4*$^{-/-}$ and *Rdh8*$^{-/-}$*Abca4*$^{-/-}$ mice, *Tlr3*$^{-/-}$*Rdh8*$^{-/-}$*Abca4*$^{-/-}$ mice displayed significantly fewer autofluorescent spots (Fig. 5, *A* and *B*). Fewer autofluorescent spots were detected in 6-month-old *Tlr3*$^{-/-}$ and WT mice as well. Appearance of these spots was noted at similar ages or just before the commencement of retinal degeneration. Age-related retinal degeneration in *Rdh8*$^{-/-}$*Abca4*$^{-/-}$ mice is seen only in the inferior retinas (4) which suggests that most of these autofluorescent spots spread throughout the entire retina are not related to deteriorated retinal structures. Increased numbers of subretinal cells were recognized by histological analysis (supplemental Fig. S3*A*), and these cells were positive for anti-macrophage/microglia antibodies (Ab) such as anti-F4/80 Ab and anti-CD11b Ab (supplemental Fig. S3*B*). These data indicate that autofluorescent spots detected by SLO represent macrophage/microglia that had migrated into the space between photoreceptors and the RPE and that lack of TLR3 delays trafficking of these cells in the retinas of *Rdh8*$^{-/-}$*Abca4*$^{-/-}$ mice. These autofluorescent spots were also observed after light exposure to *Rdh8*$^{-/-}$*Abca4*$^{-/-}$ mice (Fig. 2*B*). The brighter background-fundal autofluorescence noted in *Tlr3*$^{-/-}$*Rdh8*$^{-/-}$*Abca4*$^{-/-}$ and *Rdh8*$^{-/-}$*Abca4*$^{-/-}$ mice than in *Tlr3*$^{-/-}$ and WT mice at the age of 3 and 6 months correlated well with amounts of A2E autofluorescent deposits in the RPE (supplemental Fig. S4). Because increased numbers of macrophage/microglia into the subretinal space suggest local immune activation, the inflammatory response in the retina was also assessed by detection of glial fibrillary acid protein (GFAP), which indicates that reactive gliosis of the Muller cells reflects retinal inflammation (34). The Muller cells in 3-month-old *Rdh8*$^{-/-}$*Abca4*$^{-/-}$ mice display GFAP immunoreactivity throughout their length, whereas no obvious GFAP signal was detected in *Tlr3*$^{-/-}$*Rdh8*$^{-/-}$*Abca4*$^{-/-}$, *Tlr3*$^{-/-}$, and WT mice of the same age (Fig. 5*C* and supplemental Fig. S3*C*). This gliosis was also observed in the superior nondegenerated retina of *Rdh8*$^{-/-}$*Abca4*$^{-/-}$ mice (data not shown). These data imply the existence of inflamma-

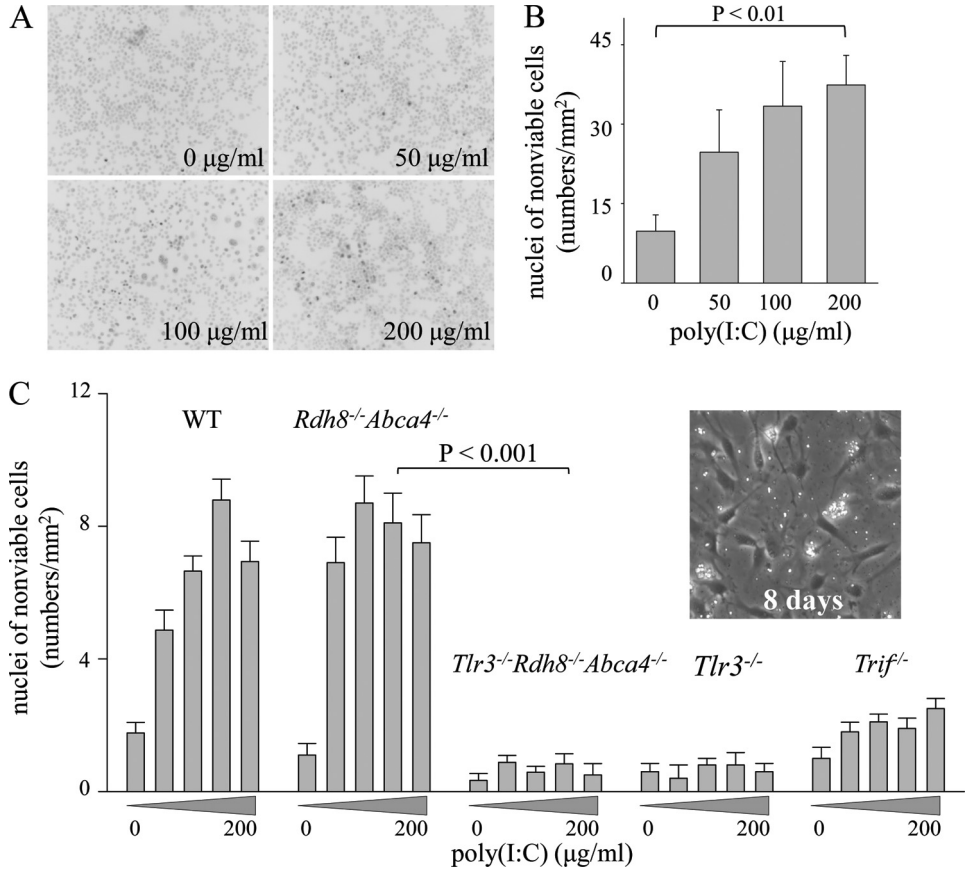

FIGURE 3. **Poly(I-C) induces death of ARPE19 cells and primary cultured RPE cells from *Rdh8*$^{-/-}$*Abca4*$^{-/-}$ and WT mice but not from *Tlr3*$^{-/-}$*Rdh8*$^{-/-}$*Abca4*$^{-/-}$, *Tlr3*$^{-/-}$, or *Trif*$^{-/-}$ mice.** *A,* ARPE19 cells (human RPE) were incubated with the TLR3 ligand, poly(I-C), at 0, 50, 100, and 200 μg/ml for 24 h and then cells were stained with Hoechst 33342. Representative ARPE19 cell images are shown. Apoptotic cells displayed chromatin condensation. *B,* numbers of chromatin condensed cells/mm^2 were counted. Poly(I-C) caused ARPE19 cell death in a dose-dependent manner. *Error bars* indicate S.D. of the means ($n > 3$). *C,* primary RPE cells were isolated from 6-week-old *Tlr3*$^{-/-}$*Rdh8*$^{-/-}$*Abca4*$^{-/-}$, *Rdh8*$^{-/-}$*Abca4*$^{-/-}$, *Tlr3*$^{-/-}$, *Trif*$^{-/-}$, and WT mice as described under "Experimental Procedures." A representative image of RPE cells after 8 days in culture is shown in the *inset*. *Numbers* of chromatin-condensed cells stained with Hoechst 33342 per mm^2 were counted. Poly(I-C)-induced cell death was observed in RPE cells from *Rdh8*$^{-/-}$*Abca4*$^{-/-}$ and WT mice after 24 h of co-incubation at 37 °C, whereas no significant cell death was detected in RPEs from *Tlr3*$^{-/-}$*Rdh8*$^{-/-}$*Abca4*$^{-/-}$ and *Tlr3*$^{-/-}$ mice ($p < 0.001$ with poly(I-C) at 100 μg/ml). RPEs from *Trif*$^{-/-}$ mice exhibited some poly(I-C)-induced cell death, but their numbers were far less than in WT mice ($p < 0.001$ at 100 μg/ml). *Error bars* indicate S.D. of the means ($n > 3$).

tory changes in the entire retina of aged *Rdh8*$^{-/-}$*Abca4*$^{-/-}$ mice and that loss of TLR3 prevents these changes.

Endogenous Components of Dying/Dead Cells Exposed to All-trans-retinal Activate TLR3—Because RPE cell impairments are well documented in macular degeneration, and because RPE cell dysfunction/death can be caused by delayed retinal clearance of all-*trans*-retinal in *Rdh8*$^{-/-}$*Abca4*$^{-/-}$ mice, we next determined if dying photoreceptors provide endogenous TLR3-activating ligands for RPE destruction. Y79 human retinoblastoma cells (1×10^5) were first incubated with all-*trans*-retinal (30 μM) for 16 h in the presence of RNase inhibitors and irradiated by UV light for 15 min, and then the supernatant containing products from damaged/dead Y79 cells was incubated with ARPE19 cells. As reported previously (29), all-*trans*-retinal caused massive Y79 cell death, and this culture supernatant contained ~120 ng/μl of DNA/RNA as measured by NanoDrop (Thermo Scientific, Waltham, MA) (supplemental Fig. S5). Irradiation with UV light for 15 min eliminated any residual all-*trans*-retinal from the supernatant (supplemental Fig. S6). After co-incubation of ARPE19 cells with this irradiated supernatant from degraded Y79 cells for 24 h, more apoptotic ARPE19 cells were observed than when ARPE19 cells were co-incubated with supernatant from live Y79 cells that had not undergone all-*trans*-retinal treatment (supplemental Fig. S7*A*). Whereas activation of NF-κB was reported when ARPE19 cells were co-incubated with supernatant containing products from either nondegraded or degraded Y79 cells, greater activation was recorded when they were co-incubated with supernatants from degraded Y79 cells (supplemental Fig. S7*B*). Moreover, ARPE19 cells overexpressing human TLR3 (hTLR3-ARPE19 cells) by 2^{15}-fold according to qPCR analysis displayed greater NF-κB activation after co-incubation with the supernatant containing products from degraded Y79 cells as well as poly(I-C) (Fig. 6*A*). HEK293 cells expressing human TLR3 (hTLR3-HEK293) also showed greater NF-κB activation than HEK293 cells after co-incubation with poly(I-C) or supernatant containing products from degraded Y79 cells (Fig. 6*B*). To examine further the TLR3 downstream signals, the interferon regulatory factor 3 (IRF3) reporter assay was performed with HEK293 cells, because TLR3 activation leads the IRF3 activation along with NF-κB. Increased IRF3 activity was shown when hTLR3-HEK293 cells were incubated with supernatant

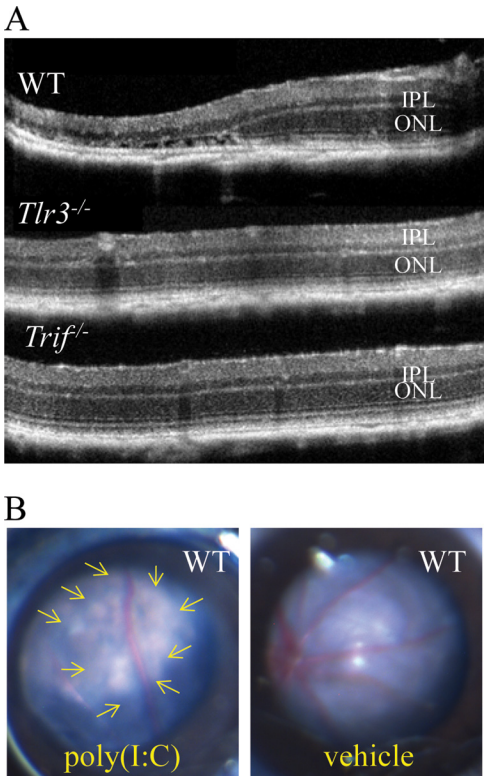

FIGURE 4. **Poly(I-C)-induced degeneration of WT retina.** Poly(I-C) (1 μl of 1 μg/μl in PBS) was injected into the subretinal space of 8-week-old WT, *Tlr3*$^{-/-}$, and *Trif*$^{-/-}$ mice. Antibiotic eye drops lacking anti-inflammatory drugs were administered to poly(I-C)- or PBS-injected eyes on day 0–3 after injection. *A,* extensively damaged retinas with loss of outer nuclear (*ONL*) and photoreceptor layers were visualized by SD-OCT in WT mice, whereas no significant changes were present in *Tlr3*$^{-/-}$ or *Trif*$^{-/-}$ mice 4 weeks after the injection. *B,* fundus images were obtained 4 weeks after poly(I-C) subretinal injection with a surgical microscope (Leica M651 MSD) connected to a CCD camera. Aberrant reflection from the cornea was removed by a HOYA HHV Dispo type-6d lens. Poly(I-C) injected WT eyes showed atrophic changes with a *pink* coloration as compared with PBS-injected WT retinas. Areas of atrophic change are indicated by *yellow arrows*.

containing products from degraded Y79 cells or poly(I-C), whereas IRF3 activity displayed reduced activity after co-incubation with the supernatant treated with Benzonase® to eliminate DNA/RNA (Fig. 6*C*). Incubation with all-*trans*-retinal (3 μM) and lipopolysaccharide (LPS) (20 μg/ml) for 6 h did not confer IRF3 activation (Fig. 6*C*). NF-κB activation in hTLR3-HEK293 cells tended to decrease in the presence of RNase A (for single-stranded RNA), RNase III (for rRNA and dsRNA), and Benzonase® (for RNA and DNA), whereas such activity was retained in the presence of RNase H (for DNA/RNA complexes) or DNase I (supplemental Fig. S5). Because macrophages are professional scavengers that express TLRs responsible for the initial defense of innate immunity, NF-κB p65 subunit nuclear translocation was examined with bone marrow-derived macrophages from *Tlr3*$^{-/-}$, *Tlr9*$^{-/-}$, *Trif*$^{-/-}$, and WT mice to determine the specificity of responses noted in cultured RPE cells. *Tlr9*$^{-/-}$ mice were employed because an endogenous chromatin (DNA)-IgG complex was reported to be a TLR9-activating ligand (35). p65 nuclear translocation by supernatants containing products from degraded Y79 cells and poly(I-C) was evidenced in macrophages from WT and *Tlr9*$^{-/-}$ mice after incubation in a dose-dependent and incubation time-dependent manner, but this translocation was not detected in macrophages from *Tlr3*$^{-/-}$ and *Trif*$^{-/-}$ mice. Benzonase® treatment, which digests DNA and RNA into stretches shorter than 5 bp in length, prevented p65 nuclear translocation in WT and *Tlr9*$^{-/-}$ mice (Fig. 6*D* and supplemental Fig. S8). These findings imply that endogenous products, most likely RNAs, from degraded photoreceptor cells function as TLR3-activating ligands.

DISCUSSION

Here, we describe a role for TLR3 in mice with age-related and acute light-induced retinal degeneration caused by disrupted all-*trans*-retinal clearance. Double knock-out mice lacking ABCA4 and RDH8 manifest CORD with hallmark features of human macular degeneration that include A2E/lipofuscin accumulation, cone/rod photoreceptor death, RPE atrophy, drusen, basal laminar deposits, thickened Bruch membrane, complement activation, and CNV. Most of these changes are displayed in the first 2–3 months of life and are exacerbated by bright light illumination (4). Obviously, rodent models do not fully recapitulate all primate structural features of the retina as they lack a macula and have significantly lower numbers of cones. Although not a perfect model for human diseases, the visual processes are still genetically/physiologically conserved among all mammalian species, and the *Rdh8*$^{-/-}$*Abca4*$^{-/-}$ mouse model develops several features shared with human macular degeneration. Thus, this and other rodent models can be used to identify and investigate pathophysiological mechanisms affecting the retina, especially because they can be genetically and environmentally manipulated.

Toll-like Receptors Are Involved in Age-related Retinal Degeneration of Rdh8$^{-/-}$*Abca4*$^{-/-}$ *Mice*—Involvement of innate immunity and chronic inflammation in pathogenesis of human macular degeneration have been suggested by evidence that includes increased AMD susceptibility of individuals with certain single nucleotide polymorphisms of key molecules involved in complement activation, and retinal changes in mice also can be related to disruption of components associated with inflammation. Although single nucleotide polymorphisms of TLR3 and TLR4 have been reported to regulate AMD susceptibility (20, 36), several conflicting reports indicating a weak relationship between AMD and these TLRs accentuate the need for studies other than single nucleotide polymorphism analyses (37–42). To examine the biological role of TLRs in retinal degeneration, we performed gene expression analyses of TLR-signaling molecules in the eyes of *Rdh8*$^{-/-}$*Abca4*$^{-/-}$ mice with age-related retinal degeneration featuring innate immune activation that included complement deposition at the Bruch membrane (4), macrophage/microglia invasion into the subretinal space, and overexpression of GFAP that indicates Muller cell activations in response to local inflammation (Fig. 5 and supplemental Fig. S3). Elevated expression of TLRs, including TLR3, was observed in 2–4-month-old *Rdh8*$^{-/-}$*Abca4*$^{-/-}$ mice with degenerating retinas and 6–8-month-old *Rdh8*$^{-/-}$*Abca4*$^{-/-}$ mice with markedly degenerated retinas with CNV. Moreover, the younger mice exhibited greater TLR signaling activity than older mice. These data suggest that TLR activation is more closely associated with photoreceptor/RPE cell death in 2–4-month-old mice and play a less dominant role in

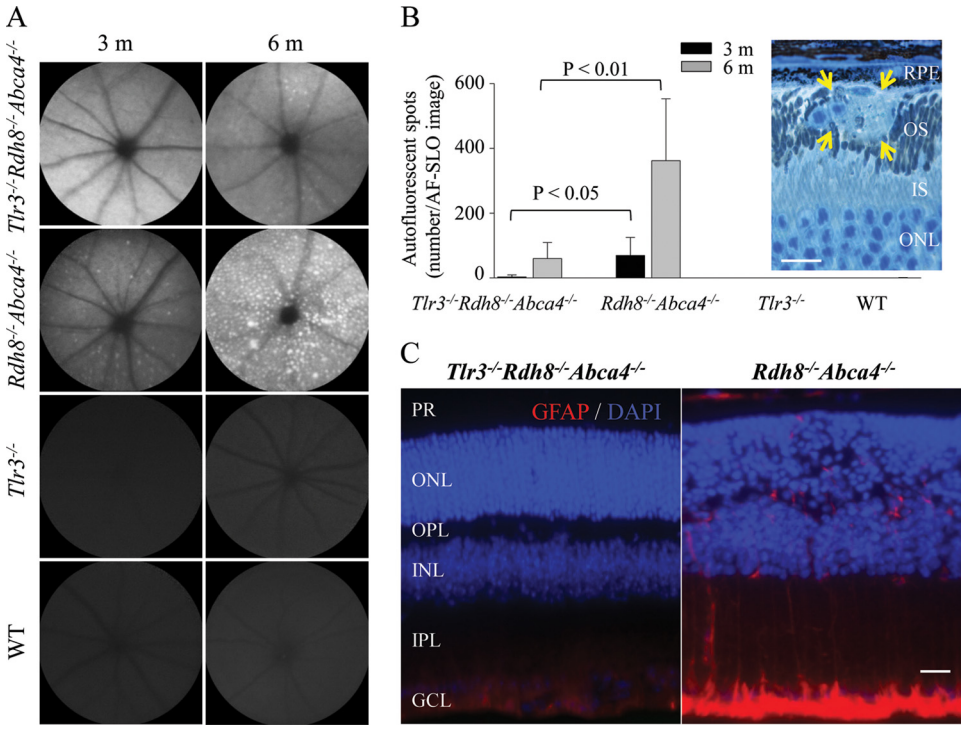

FIGURE 5. ***Tlr3*$^{-/-}$*Rdh8*$^{-/-}$*Abca4*$^{-/-}$ mice exhibit reduced numbers of autofluorescent subretinal macrophage/microglia and weaker activation of Muller glial cells.** SLO retinal images were obtained from 3- and 6-month-old *Tlr3*$^{-/-}$*Rdh8*$^{-/-}$*Abca4*$^{-/-}$, *Rdh8*$^{-/-}$*Abca4*$^{-/-}$, *Tlr3*$^{-/-}$, and WT mice (*A*), and the numbers of identified fluorescent spots are shown (*B*). Autofluorescent spots appeared in 3-month-old *Rdh8*$^{-/-}$*Abca4*$^{-/-}$ mice, and far greater numbers were noted in 6-month-old *Rdh8*$^{-/-}$*Abca4*$^{-/-}$ animals. However, *Tlr3*$^{-/-}$*Rdh8*$^{-/-}$*Abca4*$^{-/-}$ mice displayed far fewer of these spots than *Rdh8*$^{-/-}$*Abca4*$^{-/-}$ mice. Epon-prepared histological sections from 6-month-old *Rdh8*$^{-/-}$*Abca4*$^{-/-}$ mice displayed migrating macrophage/microglial cells (*yellow arrows*) in the inferior retina between photoreceptors and the RPE (*B, inset*). *OS,* outer segment; *IS,* inner segment; *ONL*, outer nuclear layer. *Bar* indicates 10 μm. *C,* expression of GFAP was examined in *Rdh8*$^{-/-}$*Abca4*$^{-/-}$ and *Tlr3*$^{-/-}$*Rdh8*$^{-/-}$*Abca4*$^{-/-}$ retinas. Cryosections from inferior retinas of 3-month-old mice were stained with anti-GFAP Ab (*red*) and DAPI (*blue*). Muller cells in 3-month-old *Rdh8*$^{-/-}$*Abca4*$^{-/-}$ mice displayed GFAP immunoreactivity throughout their length, whereas no obvious GFAP signal was detected in *Tlr3*$^{-/-}$*Rdh8*$^{-/-}$*Abca4*$^{-/-}$ mice. *PR,* photoreceptor; *ONL,* outer nuclear layer; *OPL*, outer plexiform layer; *INL,* inner nuclear layer; *IPL,* inner plexiform layer; *GCL,* ganglion cell layer. *Bar* indicates 10 μm.

the CNV formation sometimes observed in older *Rdh8*$^{-/-}$*Abca4*$^{-/-}$ mice. This observation also might explain published data indicating a stronger association of TLR3 with dry-AMD rather than wet-AMD with its characteristic CNV development (20). Notably increased expression of TLR3, TRIF, and the CXCL10 chemokine was also manifest in older WT mice compared with younger WT mice. Together with evidence of macrophage/microglia infiltration into the subretinal space of older WT mice (data not shown) (31), our array analyses strongly support an important role for chronic inflammation in normal aging and the pathology of age-related retinal degeneration in mice.

TLR3 Activation Causes Inflammation and RPE Death—Activation of TLRs induces expression of type 1- cytokines such as IFNs and ILs that eventually activate pathways involved in inflammation and cell apoptosis (27). The TLR3-activating ligand dsRNA has been reported to induce apoptosis of several cell types through multiple pathways (43, 44). TLR3 activation also may directly trigger apoptosis of cancer cells (45) and human RPE cells (20). The most recent study demonstrated pro-apoptotic activity of TLR3/TRIF/caspase-8 in melanoma cells (30). In this study, poly(I-C) caused caspase-8 cleavage in HEK293 cells, but caspase-8 expression was not detected in ARPE19 cells. Instead, ARPE19 cells displayed Bax-associated and caspase-8-independent apoptosis (supplemental Fig. S1). Poly(I-C)-induced cell death was observed in human RPE (ARPE19) cells and primary RPE cells from *Rdh8*$^{-/-}$*Abca4*$^{-/-}$ and WT mice but not in RPE cells from *Tlr3*$^{-/-}$*Rdh8*$^{-/-}$*Abca4*$^{-/-}$ and *Tlr3*$^{-/-}$ mice (Fig. 3). Importantly, RPE cell death was caused by products released from degenerated retinal cells killed by all-*trans*-retinal toxicity. By inducing mitochondria-associated apoptosis (29, 46), all-*trans*-retinal is directly toxic to cells. Our array analyses demonstrated activation of several TLRs in age-related retinal degeneration of *Rdh8*$^{-/-}$ *Abca4*$^{-/-}$ mice (Table 1), and the products released from these degenerating retinal cells might activate other TLRs and/or inflammatory pathways. Indeed, increasing evidence for TLR-mediated diseases and identification of endogenous ligands for TLRs have been reported (18, 47, 48). The significant increase of NF-κB activation in ARPE19 cells co-incubated with supernatants from UV-illuminated and all-*trans*-retinal-untreated live Y79 cells also suggest an inflammatory reaction caused by a different underlying mechanism (supplemental Fig. S7*B*). Although inflammation initiated by TLR3 might be involved in RPE death, several observations in this study indicate that TLR3 activation is a major contributor to this pathology. These include data showing that primary RPE cells from *Rdh8*$^{-/-}$*Abca4*$^{-/-}$ and WT mice underwent poly(I-C)-induced death, although this was not observed in RPE cells from *Tlr3*$^{-/-}$*Rdh8*$^{-/-}$*Abca4*$^{-/-}$ and *Tlr3*$^{-/-}$ mice (Fig. 3*C*). Furthermore, activation of NF-κB and IRF3 in cultured cells with overexpressed TLR3 was greater than in control cells (Fig. 6, *A–C*), and decreased NF-κB and IRF3 activation was documented in the presence of RNase A, RNase III, or Benzonase® (Fig. 6*C* and supplemental Fig. S5*B*). Notably, nuclear

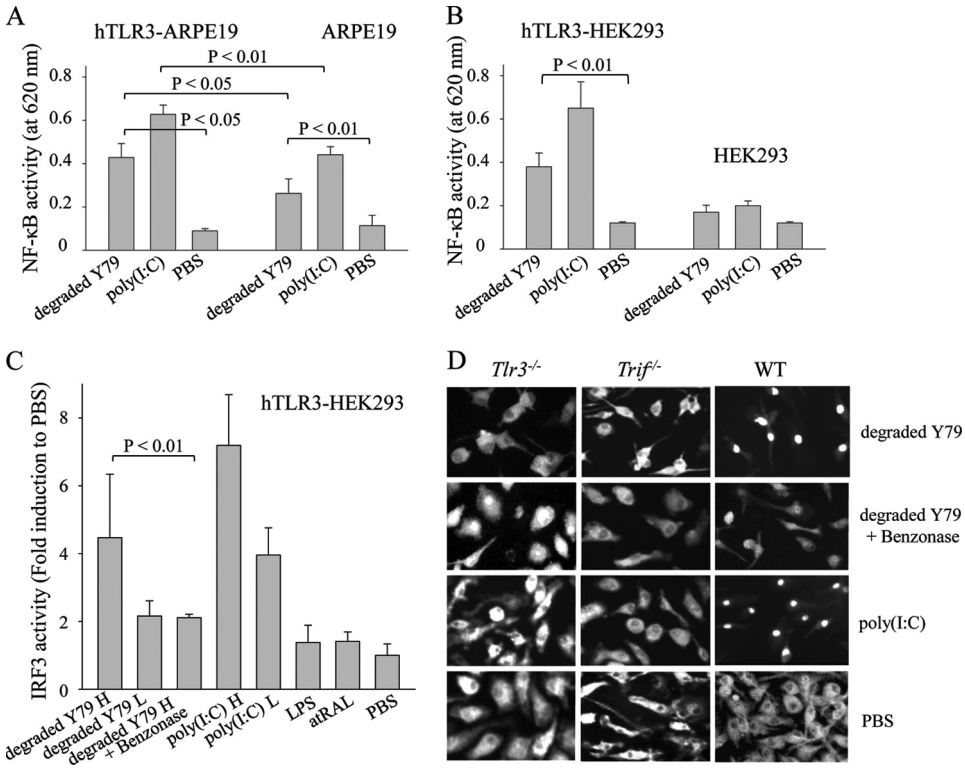

FIGURE 6. **Endogenous products emanating from photoreceptor cells co-incubated with all-*trans*-retinal activate TLR3.** *A,* ARPE19 and ARPE19 cells with overexpressed hTLR3 (hTLR3-ARPE19 cells) were co-incubated with supernatants containing products from degraded Y79 cells (20 μl of the supernatant in 40 μl of HEK-Blue detection media) or poly(I-C) (50 μg/ml) in 96-well plates, and reporter activity of NF-κB was evaluated after 6 h of co-incubation at 37 °C by monitoring absorbance of the detection media at 620 nm. *Error bars* indicate S.D. of the means ($n > 3$). *B,* reporter activity of NF-κB was also measured for HEK293 cells with and without overexpressed hTLR3 (hTLR3-HEK293) co-incubated with supernatants containing products from degraded Y79 cells (20 μl of the supernatant in 40 μl of HEK-Blue detection media) or poly(I-C) (50 μg/ml) in 96-well plates. Absorbance was monitored at 620 nm after 16 h of co-incubation at 37 °C. *Error bars* indicate S.D. of the means ($n > 3$). *C,* reporter activity of IFR3 was measured with a luciferase assay for hTLR3-HEK293 co-incubated with supernatants containing products from degraded Y79 cells (200 μl (*H*) or 40 μl (*L*) of the supernatant in 300 or 460 μl of media), supernatants containing products from degraded Y79 cells (200 μl of the supernatant in 300 μl of media), pretreated with Benzonase® (20 units/ml) for 1 h, and heated at 70 °C for 5 min to deactivate the enzyme, poly(I-C) (50 μg/ml (*H*) or 10 μg/ml (*L*)), lipopolysaccharide (*LPS* at 10 μg/ml), or all-*trans*-retinal (3 μM) in 24-well plates. Luciferase activity was measured after 6 h of co-incubation at 37 °C, and fold changes to PBS-treated cells were calculated. *Error bars* indicate S.D. of the means ($n > 3$). *D,* NF-κB p65 subunit nuclear translocation was examined with bone marrow-derived macrophages from *Tlr3*$^{-/-}$, *Trif*$^{-/-}$, and WT mice after incubation with supernatants containing products from degraded Y79 cells (the supernatant without any dilution), supernatants containing products from degraded Y79 cells pretreated with Benzonase® (20 units/ml) for 1 h and heated at 70 °C for 5 min to deactivate the enzyme or poly(I-C) (10 μg/ml) for 2 h. Supernatants containing products from degraded Y79 cells and poly(I-C) induced p65 nuclear translocation, but Bensonase® treatment prevented this translocation in WT macrophages. Bone marrow-derived macrophages from *Tlr3*$^{-/-}$ and *Trif*$^{-/-}$ mice failed to translocate the p65 subunit.

translocation of NF-κB p65 was diminished by Benzonase® treatment to eliminate DNA and RNA (Fig. 6*D* and supplemental Fig. S8), and macrophages from *Tlr9*$^{-/-}$ mice displayed p65 translocation similar to WT macrophages. Together, these data indicate that endogenous RNA from photoreceptors degraded by all-*trans*-retinal induced TLR3-dependent inflammation and cell death. Several lines of evidence support this concept. First, RNA released from rapidly degraded cells was found to be an endogenous TLR3 ligand (49). Second, mRNA from necrotic cells can activate TLR3 (50). Third, RNA-induced immune activation occurs due to autoantibodies against DNA and RNA in patients with systemic lupus erythematosus. Fourth, there is a predominance of neuronal mRNA in Alzheimer plaques (51, 52), and reduced transcription of TLRs, including TLR3, was exhibited by mononuclear cells of patients with Alzheimer disease (53). Recent studies also support existence of endogenous dsRNA present in the retina as microRNAs (54–56). In acute light-induced retinal degeneration, nucleic acid-related deposits in the photoreceptor layer were formed that stained with DAPI, Hoechst dyes, and Sytox dye, which together with toluidine blue recognize nucleic acids (57), all suggesting the presence of dsRNA-like endogenous products during this type of tissue degeneration. These data indicate that TLR3 plays a role in both chronic inflammation and ligand-induced RPE/photoreceptor cell death in human retinal diseases.

TLR3 Involvement in the Development of Retinopathy in Rdh8$^{-/-}$*Abca4*$^{-/-}$ *Mice*—Although *Rdh8*$^{-/-}$*Abca4*$^{-/-}$ mice exhibit two different phenotypes of retinal degeneration, namely age-related degeneration (evidenced by CORD) and bright light-induced acute retinal degeneration, both phenotypes initially show a delayed clearance of all-*trans*-retinal (4). Toxicity of all-*trans*-retinal as a reactive aldehyde includes increased cell permeability and mitochondrial impairment (29). Accumulated conjugates of all-*trans*-retinal, A2E, and all-*trans*-retinal dimer that can induce RPE death by oxidative stress and inhibit RPE phagocytosis (58, 59) were observed *in vitro* and in animal investigations. Amounts of accumulated A2E directly reflect the quantity of all-*trans*-retinal formation during the retinoid cycle. Interestingly, although ablating TLR3 ameliorated age-related retinal degeneration in *Rdh8*$^{-/-}$

Abca4$^{-/-}$ mice, *Tlr3*$^{-/-}$*Rdh8*$^{-/-}$*Abca4*$^{-/-}$ mice still exhibited impaired macrophage/microglia infiltration without changes in A2E accumulation, indicating that modulation of chronic immune responses (with no changes in the all-*trans*-retinal levels) due to loss of TLR3 is associated with age-related retinal degeneration in mice. Our qPCR demonstrated no elevation of TLR3 expression in ARPE19 cells after co-incubation with all-*trans*-retinal and A2E, whereas poly(I-C) caused increased expression of TLR3 (data not shown), suggesting that retinoids are not likely to serve as TLR3-activating ligands.

In addition to increased expression of TLRs in CORD (Table 1), a 2-fold increase in TLR3 expression was noted in *Rdh8*$^{-/-}$*Abca4*$^{-/-}$ mice with acute retinal degeneration after bright light exposure (Fig. 2*C*). But retinal degeneration in *Tlr3*$^{-/-}$*Rdh8*$^{-/-}$*Abca4*$^{-/-}$ mice was far less severe than in *Rdh8*$^{-/-}$*Abca4*$^{-/-}$ mice exposed to 15 and 30 min of 10,000 lux illumination (Fig. 2, *A* and *B*). Together, these observations indicate a role of TLR3 in acute and chronic degeneration in *Rdh8*$^{-/-}$*Abca4*$^{-/-}$ mice. However, retinal damage was similar in *Rdh8*$^{-/-}$*Abca4*$^{-/-}$ and *Tlr3*$^{-/-}$*Rdh8*$^{-/-}$*Abca4*$^{-/-}$ mice after the 60-min bright light exposure. This observation suggests that TLR3-associated retinal degeneration may be reduced in milder lighting environments, but other cell death mechanisms, such those induced by oxidative stress, may predominate after extensive exposure to bright light.

Relevance of the Findings in This Study to Human AMD—AMD is an etiologically complex disease wherein multiple genetic and environmental factors influence disease progression. Genes encoding complement factor H (7–14), HtrA serine peptidase 1 (HTRA1) (60–63), and complement components 2 and 3 (C2 and C3) (15, 16) were reported to predispose to AMD, and both human and mouse studies have demonstrated complement deposition at AMD lesions (64–66). In addition, the F412L polymorphism of TLR3 (20) and the D299G of TLR4 (36) have been reported, but these findings were refuted by multiple groups (37–42). Thus, there is an emerging consensus that innate immunity plays an important role in the pathogenesis of AMD. Indeed, recent animal studies indicate that perturbed immune responses are associated with retinal changes. Immunization of mice with carboxyethylpyrrole-modified mouse serum albumin induced a retinopathy with a phenotype similar to dry-AMD (66). Targeted deletion of genes encoding either monocyte chemoattractant protein-1 (CCL2), C-C chemokine receptor-2 (CCR2), or CX3C chemokine receptor-1 (CX3CR1) mimicked some features of AMD in mice. *Ccl2*$^{-/-}$*Ccr2*$^{-/-}$ mice in particular have been accepted as AMD model animals (65, 67, 68); however, the latest characterization of *Ccl2*$^{-/-}$ mice indicates that most of the described hallmarks of AMD in these mice can be explained by normal aging (31). Mice with a knock-out of complement factor H (*Cfh*$^{-/-}$) showed only thinning of Bruch membrane, lipofuscin deposition, and disorganized photoreceptor outer segments at the advanced age of 24 months (69). Although the pathology of AMD very likely involves inflammatory reactions, the molecular mechanisms that induce them remain largely unknown. In this study, enhanced TLR-signaling was observed in age-related retinal degeneration in *Rdh8*$^{-/-}$*Abca4*$^{-/-}$ mice. We also found that TLR3 is expressed in human and mouse RPE and that RPE cell death is induced via TLR3 by endogenous products of all-*trans*-retinal-exposed photoreceptor cells in addition to synthetic dsRNA. Importantly, *Tlr3*$^{-/-}$*Rdh8*$^{-/-}$*Abca4*$^{-/-}$ mice did not develop age-related or bright light-induced retinal degeneration in the absence of TLR3. We therefore conclude that TLR3 plays an important role in all-*trans*-retinal-associated retinal degeneration in mice and that it is a potential target for therapies directed at ameliorating human retinal degeneration, including Stargardt disease and AMD. This work represents the first study linking retinopathies emanating from aberrant function of the retinoid cycle to the immunological mechanisms ascribed to human Stargardt disease and AMD.

Acknowledgments—We thank Drs. L. T. Webster, Jr., K. Ishikawa, V. Chauhan, S. Matsuyama, M. S. Matosky, and S. Roos (Case Western Reserve University) for their comments and technical support.

REFERENCES

1. Palczewski, K. (2006) *Annu. Rev. Biochem.* **75,** 743–767
2. Travis, G. H., Golczak, M., Moise, A. R., and Palczewski, K. (2007) *Annu. Rev. Pharmacol. Toxicol.* **47,** 469–512
3. von Lintig, J., Kiser, P. D., Golczak, M., and Palczewski, K. (2010) *Trends Biochem. Sci.* **35,** 400–410
4. Maeda, A., Maeda, T., Golczak, M., and Palczewski, K. (2008) *J. Biol. Chem.* **283,** 26684–26693
5. Allikmets, R., Singh, N., Sun, H., Shroyer, N. F., Hutchinson, A., Chidambaram, A., Gerrard, B., Baird, L., Stauffer, D., Peiffer, A., Rattner, A., Smallwood, P., Li, Y., Anderson, K. L., Lewis, R. A., Nathans, J., Leppert, M., Dean, M., and Lupski, J. R. (1997) *Nat. Genet.* **15,** 236–246
6. Allikmets, R. (2000) *Am. J. Hum. Genet.* **67,** 487–491
7. Haines, J. L., Hauser, M. A., Schmidt, S., Scott, W. K., Olson, L. M., Gallins, P., Spencer, K. L., Kwan, S. Y., Noureddine, M., Gilbert, J. R., Schnetz-Boutaud, N., Agarwal, A., Postel, E. A., and Pericak-Vance, M. A. (2005) *Science* **308,** 419–421
8. Edwards, A. O., Ritter, R., 3rd, Abel, K. J., Manning, A., Panhuysen, C., and Farrer, L. A. (2005) *Science* **308,** 421–424
9. Yates, J. R., Sepp, T., Matharu, B. K., Khan, J. C., Thurlby, D. A., Shahid, H., Clayton, D. G., Hayward, C., Morgan, J., Wright, A. F., Armbrecht, A. M., Dhillon, B., Deary, I. J., Redmond, E., Bird, A. C., and Moore, A. T. (2007) *N. Engl. J. Med.* **357,** 553–561
10. Hageman, G. S., Anderson, D. H., Johnson, L. V., Hancox, L. S., Taiber, A. J., Hardisty, L. I., Hageman, J. L., Stockman, H. A., Borchardt, J. D., Gehrs, K. M., Smith, R. J., Silvestri, G., Russell, S. R., Klaver, C. C., Barbazetto, I., Chang, S., Yannuzzi, L. A., Barile, G. R., Merriam, J. C., Smith, R. T., Olsh, A. K., Bergeron, J., Zernant, J., Merriam, J. E., Gold, B., Dean, M., and Allikmets, R. (2005) *Proc. Natl. Acad. Sci. U.S.A.* **102,** 7227–7232
11. Hughes, A. E., Orr, N., Esfandiary, H., Diaz-Torres, M., Goodship, T., and Chakravarthy, U. (2006) *Nat. Genet.* **38,** 1173–1177
12. Klein, R. J., Zeiss, C., Chew, E. Y., Tsai, J. Y., Sackler, R. S., Haynes, C., Henning, A. K., SanGiovanni, J. P., Mane, S. M., Mayne, S. T., Bracken, M. B., Ferris, F. L., Ott, J., Barnstable, C., and Hoh, J. (2005) *Science* **308,** 385–389
13. Maller, J., George, S., Purcell, S., Fagerness, J., Altshuler, D., Daly, M. J., and Seddon, J. M. (2006) *Nat. Genet.* **38,** 1055–1059
14. Magnusson, K. P., Duan, S., Sigurdsson, H., Petursson, H., Yang, Z., Zhao, Y., Bernstein, P. S., Ge, J., Jonasson, F., Stefansson, E., Helgadottir, G., Zabriskie, N. A., Jonsson, T., Björnsson, A., Thorlacius, T., Jonsson, P. V., Thorleifsson, G., Kong, A., Stefansson, H., Zhang, K., Stefansson, K., and Gulcher, J. R. (2006) *PLoS Med.* **3,** e5
15. Maller, J. B., Fagerness, J. A., Reynolds, R. C., Neale, B. M., Daly, M. J., and Seddon, J. M. (2007) *Nat. Genet.* **39,** 1200–1201
16. Gold, B., Merriam, J. E., Zernant, J., Hancox, L. S., Taiber, A. J., Gehrs, K., Cramer, K., Neel, J., Bergeron, J., Barile, G. R., Smith, R. T., Hageman, G. S., Dean, M., and Allikmets, R. (2006) *Nat. Genet.* **38,** 458–462
17. Medzhitov, R. (2008) *Nature* **454,** 428–435

18. Kawai, T., and Akira, S. (2010) *Nat. Immunol.* **11,** 373–384
19. Kumar, M. V., Nagineni, C. N., Chin, M. S., Hooks, J. J., and Detrick, B. (2004) *J. Neuroimmunol.* **153,** 7–15
20. Yang, Z., Stratton, C., Francis, P. J., Kleinman, M. E., Tan, P. L., Gibbs, D., Tong, Z., Chen, H., Constantine, R., Yang, X., Chen, Y., Zeng, J., Davey, L., Ma, X., Hau, V. S., Wang, C., Harmon, J., Buehler, J., Pearson, E., Patel, S., Kaminoh, Y., Watkins, S., Luo, L., Zabriskie, N. A., Bernstein, P. S., Cho, W., Schwager, A., Hinton, D. R., Klein, M. L., Hamon, S. C., Simmons, E., Yu, B., Campochiaro, B., Sunness, J. S., Campochiaro, P., Jorde, L., Parmigiani, G., Zack, D. J., Katsanis, N., Ambati, J., and Zhang, K. (2008) *N. Engl. J. Med.* **359,** 1456–1463
21. Kleinman, M. E., Yamada, K., Takeda, A., Chandrasekaran, V., Nozaki, M., Baffi, J. Z., Albuquerque, R. J., Yamasaki, S., Itaya, M., Pan, Y., Appukuttan, B., Gibbs, D., Yang, Z., Karikó, K., Ambati, B. K., Wilgus, T. A., DiPietro, L. A., Sakurai, E., Zhang, K., Smith, J. R., Taylor, E. W., and Ambati, J. (2008) *Nature* **452,** 591–597
22. Deleidi, M., Hallett, P. J., Koprich, J. B., Chung, C. Y., and Isacson, O. (2010) *J. Neurosci.* **30,** 16091–16101
23. Maeda, A., Maeda, T., Imanishi, Y., Kuksa, V., Alekseev, A., Bronson, J. D., Zhang, H., Zhu, L., Sun, W., Saperstein, D. A., Rieke, F., Baehr, W., and Palczewski, K. (2005) *J. Biol. Chem.* **280,** 18822–18832
24. Sonoda, S., Spee, C., Barron, E., Ryan, S. J., Kannan, R., and Hinton, D. R. (2009) *Nat. Protoc.* **4,** 662–673
25. Parish, C. A., Hashimoto, M., Nakanishi, K., Dillon, J., and Sparrow, J. (1998) *Proc. Natl. Acad. Sci. U.S.A.* **95,** 14609–14613
26. Johnson, A. C., Li, X., and Pearlman, E. (2008) *J. Biol. Chem.* **283,** 3988–3996
27. Kawai, T., and Akira, S. (2008) *Ann. N.Y. Acad. Sci.* **1143,** 1–20
28. Glenn, J. V., Mahaffy, H., Wu, K., Smith, G., Nagai, R., Simpson, D. A., Boulton, M. E., and Stitt, A. W. (2009) *Invest. Ophthalmol. Vis. Sci.* **50,** 441–451
29. Maeda, A., Maeda, T., Golczak, M., Chou, S., Desai, A., Hoppel, C. L., Matsuyama, S., and Palczewski, K. (2009) *J. Biol. Chem.* **284,** 15173–15183
30. Weber, A., Kirejczyk, Z., Besch, R., Potthoff, S., Leverkus, M., and Häcker, G. (2010) *Cell Death Differ.* **17,** 942–951
31. Luhmann, U. F., Robbie, S., Munro, P. M., Barker, S. E., Duran, Y., Luong, V., Fitzke, F. W., Bainbridge, J. W., Ali, R. R., and MacLaren, R. E. (2009) *Invest. Ophthalmol. Vis. Sci.* **50,** 5934–5943
32. Joly, S., Francke, M., Ulbricht, E., Beck, S., Seeliger, M., Hirrlinger, P., Hirrlinger, J., Lang, K. S., Zinkernagel, M., Odermatt, B., Samardzija, M., Reichenbach, A., Grimm, C., and Remé, C. E. (2009) *Am. J. Pathol.* **174,** 2310–2323
33. Hoh Kam, J., Lenassi, E., and Jeffery, G. (2010) *PloS One* **5,** e13127
34. Bringmann, A., Pannicke, T., Grosche, J., Francke, M., Wiedemann, P., Skatchkov, S. N., Osborne, N. N., and Reichenbach, A. (2006) *Prog. Retin. Eye Res.* **25,** 397–424
35. Leadbetter, E. A., Rifkin, I. R., Hohlbaum, A. M., Beaudette, B. C., Shlomchik, M. J., and Marshak-Rothstein, A. (2002) *Nature* **416,** 603–607
36. Zareparsi, S., Buraczynska, M., Branham, K. E., Shah, S., Eng, D., Li, M., Pawar, H., Yashar, B. M., Moroi, S. E., Lichter, P. R., Petty, H. R., Richards, J. E., Abecasis, G. R., Elner, V. M., and Swaroop, A. (2005) *Hum. Mol. Genet.* **14,** 1449–1455
37. Lewin, A. S. (2009) *N. Engl. J. Med.* **360,** 2251–2256
38. Liew, G., Mitchell, P., and Wong, T. Y. (2009) *N. Engl. J. Med.* **360,** 2252
39. Edwards, A. O., Swaroop, A., and Seddon, J. M. (2009) *N. Engl. J. Med.* **360,** 2254–2255
40. Allikmets, R., Bergen, A. A., Dean, M., Guymer, R. H., Hageman, G. S., Klaver, C. C., Stefansson, K., and Weber, B. H. (2009) *N. Engl. J. Med.* **360,** 2252–2254
41. Cho, Y., Wang, J. J., Chew, E. Y., Ferris, F. L., 3rd, Mitchell, P., Chan, C. C., and Tuo, J. (2009) *Invest. Ophthalmol. Vis. Sci.* **50,** 5614–5618
42. Edwards, A. O., Chen, D., Fridley, B. L., James, K. M., Wu, Y., Abecasis, G., Swaroop, A., Othman, M., Branham, K., Iyengar, S. K., Sivakumaran, T. A., Klein, R., Klein, B. E., and Tosakulwong, N. (2008) *Invest. Ophthalmol. Vis. Sci.* **49,** 1652–1659
43. Weber, A., Kirejczyk, Z., Besch, R., Potthoff, S., Leverkus, M., and Hacker, G. (2009) *Cell Death Differ.* **17,** 942–951
44. Yoneda, K., Sugimoto, K., Shiraki, K., Tanaka, J., Beppu, T., Fuke, H., Yamamoto, N., Masuya, M., Horie, R., Uchida, K., and Takei, Y. (2008) *Int. J. Oncol.* **33,** 929–936
45. Salaun, B., Coste, I., Rissoan, M. C., Lebecque, S. J., and Renno, T. (2006) *J. Immunol.* **176,** 4894–4901
46. Sparrow, J. R., Wu, Y., Kim, C. Y., and Zhou, J. (2010) *J. Lipid Res.* **51,** 247–261
47. Liew, F. Y., Xu, D., Brint, E. K., and O'Neill, L. A. (2005) *Nat. Rev. Immunol.* **5,** 446–458
48. West, X. Z., Malinin, N. L., Merkulova, A. A., Tischenko, M., Kerr, B. A., Borden, E. C., Podrez, E. A., Salomon, R. G., and Byzova, T. V. (2010) *Nature* **467,** 972–976
49. Karikó, K., Ni, H., Capodici, J., Lamphier, M., and Weissman, D. (2004) *J. Biol. Chem.* **279,** 12542–12550
50. Cavassani, K. A., Ishii, M., Wen, H., Schaller, M. A., Lincoln, P. M., Lukacs, N. W., Hogaboam, C. M., and Kunkel, S. L. (2008) *J. Exp. Med.* **205,** 2609–2621
51. Eilat, D., and Anderson, W. F. (1994) *Mol. Immunol.* **31,** 1377–1390
52. Ginsberg, S. D., Crino, P. B., Hemby, S. E., Weingarten, J. A., Lee, V. M., Eberwine, J. H., and Trojanowski, J. Q. (1999) *Ann. Neurol.* **45,** 174–181
53. Fiala, M., Liu, P. T., Espinosa-Jeffrey, A., Rosenthal, M. J., Bernard, G., Ringman, J. M., Sayre, J., Zhang, L., Zaghi, J., Dejbakhsh, S., Chiang, B., Hui, J., Mahanian, M., Baghaee, A., Hong, P., and Cashman, J. (2007) *Proc. Natl. Acad. Sci. U.S.A.* **104,** 12849–12854
54. Arora, A., Guduric-Fuchs, J., Harwood, L., Dellett, M., Cogliati, T., and Simpson, D. A. (2010) *BMC Dev. Biol.* **10,** 1
55. Loscher, C. J., Hokamp, K., Kenna, P. F., Ivens, A. C., Humphries, P., Palfi, A., and Farrar, G. J. (2007) *Genome Biol.* **8,** R248
56. Ryan, D. G., Oliveira-Fernandes, M., and Lavker, R. M. (2006) *Mol. Vis.* **12,** 1175–1184
57. Maeda, A., Okano, K., Park, P. S., Lem, J., Crouch, R. K., Maeda, T., and Palczewski, K. (2010) *Proc. Natl. Acad. Sci. U.S.A.* **107,** 8428–8433
58. Sparrow, J. R., and Cai, B. (2001) *Invest. Ophthalmol. Vis. Sci.* **42,** 1356–1362
59. Vives-Bauza, C., Anand, M., Shirazi, A. K., Magrane, J., Gao, J., Vollmer-Snarr, H. R., Manfredi, G., and Finnemann, S. C. (2008) *J. Biol. Chem.* **283,** 24770–24780
60. Jakobsdottir, J., Conley, Y. P., Weeks, D. E., Mah, T. S., Ferrell, R. E., and Gorin, M. B. (2005) *Am. J. Hum. Genet.* **77,** 389–407
61. Rivera, A., Fisher, S. A., Fritsche, L. G., Keilhauer, C. N., Lichtner, P., Meitinger, T., and Weber, B. H. (2005) *Hum. Mol. Genet.* **14,** 3227–3236
62. Yang, Z., Camp, N. J., Sun, H., Tong, Z., Gibbs, D., Cameron, D. J., Chen, H., Zhao, Y., Pearson, E., Li, X., Chien, J., Dewan, A., Harmon, J., Bernstein, P. S., Shridhar, V., Zabriskie, N. A., Hoh, J., Howes, K., and Zhang, K. (2006) *Science* **314,** 992–993
63. Dewan, A., Liu, M., Hartman, S., Zhang, S. S., Liu, D. T., Zhao, C., Tam, P. O., Chan, W. M., Lam, D. S., Snyder, M., Barnstable, C., Pang, C. P., and Hoh, J. (2006) *Science* **314,** 989–992
64. Mullins, R. F., Russell, S. R., Anderson, D. H., and Hageman, G. S. (2000) *FASEB J.* **14,** 835–846
65. Ambati, J., Anand, A., Fernandez, S., Sakurai, E., Lynn, B. C., Kuziel, W. A., Rollins, B. J., and Ambati, B. K. (2003) *Nat. Med.* **9,** 1390–1397
66. Hollyfield, J. G., Bonilha, V. L., Rayborn, M. E., Yang, X., Shadrach, K. G., Lu, L., Ufret, R. L., Salomon, R. G., and Perez, V. L. (2008) *Nat. Med.* **14,** 194–198
67. Shen, D., Wen, R., Tuo, J., Bojanowski, C. M., and Chan, C. C. (2006) *Ophthalmic Res.* **38,** 71–73
68. Combadière, C., Feumi, C., Raoul, W., Keller, N., Rodéro, M., Pézard, A., Lavalette, S., Houssier, M., Jonet, L., Picard, E., Debré, P., Sirinyan, M., Deterre, P., Ferroukhi, T., Cohen, S. Y., Chauvaud, D., Jeanny, J. C., Chemtob, S., Behar-Cohen, F., and Sennlaub, F. (2007) *J. Clin. Invest.* **117,** 2920–2928
69. Coffey, P. J., Gias, C., McDermott, C. J., Lundh, P., Pickering, M. C., Sethi, C., Bird, A., Fitzke, F. W., Maass, A., Chen, L. L., Holder, G. E., Luthert, P. J., Salt, T. E., Moss, S. E., and Greenwood, J. (2007) *Proc. Natl. Acad. Sci. U.S.A.* **104,** 16651–16656